HHS Public Access

Author manuscript

Hepatology. Author manuscript; available in PMC 2020 June 24.

The role of 3D-MRE in the diagnosis of NASH in obese patients undergoing bariatric surgery

Alina M. Allen, MD[1] **[Assistant Professor of Medicine]**, **Vijay H. Shah, MD**[1] **[Professor of Medicine and Physiology]**, **Terry M. Therneau, PhD**[2] **[Professor of Biostatistics]**, **Sudhakar K. Venkatesh, MD**[3] **[Professor of Radiology]**, **Taofic Mounajjed, MD**[4] **[Assistant Professor of Laboratory Medicine and Pathology]**, **Joseph J. Larson**[2] **[Instructor in Biostatistics]**, **Kristin C. Mara**[2] **[Statistician I]**, **Phillip J. Schulte, PhD**[2] **[Assistant Professor of Biostatistics]**, **Todd A. Kellogg, MD**[5] **[Assistant Professor of Surgery]**, **Michael L. Kendrick, MD**[5] **[Professor of Surgery]**, **Travis J. McKenzie, MD**[5] **[Assistant Professor of Surgery]**, **Suzanne M. Greiner**[1] **[Associate Clinical Research Coordinator]**, **Jiahui Li, MD**[3] **[Research fellow]**, **Kevin J. Glaser, PhD**[3] **[Instructor in Medical Physics]**, **Michael L. Wells, MD**[3] **[Assistant Professor of Radiology]**, **Jun Chen, PhD**[3] **[Assistant Professor of Radiology]**, **Richard L. Ehman, MD**[3] **[Professor of Radiology]**, and **Meng Yin, PhD**[3] **[Associate Professor of Medical Physics]**

[1]Division of Gastroenterology and Hepatology, Mayo Clinic, Rochester, MN

[2]Department of Biomedical Statistics and Informatics, Mayo Clinic, Rochester, MN

[3]Department of Radiology, Mayo Clinic, Rochester, MN

[4]Division of Anatomic Pathology, Mayo Clinic, Rochester, MN

[5]Division of Metabolic Surgery, Mayo Clinic, Rochester, MN

Abstract

The lack of reliable, noninvasive methods to diagnose early nonalcoholic steatohepatitis (NASH) is a major unmet need. We aimed to determine the diagnostic accuracy of 3D-MRE, with shear stiffness measured at 60 Hz, damping ratio at 40 Hz, and MRI proton density fat fraction (MRI-PDFF) in the detection of NASH in individuals undergoing bariatric surgery. Obese adults at risk for NASH were enrolled between 2015-2017 (prospective cohort, n=88) and 2010-2013 (retrospective cohort, n=87). The imaging protocol consisted of multifrequency 3D-MRE (mf3D-MRE) with shear waves delivered at different frequencies to explore parameters that best correlated with histologic NASH; and MRI-PDFF to estimate steatosis. The prospective cohort was used to establish the optimal mf3D-MRE technical parameters for NASH detection. The 2 cohorts were then combined to derive predictive models of NASH and disease activity by NAFLD activity score (NAS) using the 3 imaging parameters that correlated with NASH. A total of 175 patients, median age 45, 81% women, and 81 (46%) with histologic NASH were used for model

Corresponding author: Meng Yin, PhD, Department of Radiology , Mayo Clinic, 200 First Street SW, Rochester MN 55905, yin.meng@mayo.edu, Telephone: 507-284-9777, Fax: 507-284-9778.

Conflict of interest

The Mayo Clinic and Drs. Ehman and Yin have intellectual property and a financial interest related to this research. This research has been reviewed by the Mayo Clinic Conflict of Interest Review Board as is being conducted in compliance with Mayo Clinic Conflict of Interest policies.

derivation. From the complex shear modulus output generated by mf3D-MRE, the *damping ratio* at 40Hz and *shear stiffness* at 60Hz best correlated with NASH. The *fat fraction* obtained from MRI-PDFF correlated with steatosis ($p<0.05$ for all). These 3 parameters were fit into a logistic regression model which predicted NASH with cross-validated AUROC=0.73, sensitivity=0.67, specificity= 0.80, PPV= 0.73 and NPV=0.74 and disease activity by NAS with cross-validated AUROC=0.82.

Conclusion: Multifrequency 3D-MRE allows identification of novel imaging parameters that predict early NASH and disease activity. This imaging biomarker represents a promising alternative to liver biopsy for NASH diagnosis and monitoring. The results provide motivation for further studies in non-bariatric cohorts. ClinicalTrials.gov number, NCT02565446.

Keywords

NAFLD; biomarker; diagnosis; noninvasive

Chronic liver disease is one of the key contributors to the recent decrease in life expectancy in the United States(1). Among causes of chronic liver disease, nonalcoholic fatty liver disease (NAFLD) is the most common, with an estimated worldwide prevalence ranging from 25% to 45%(2). In the US, it is estimated that 75-100 million individuals are affected and the incidence continues to increase(3). Approximately 20-25% of NAFLD patients develop nonalcoholic steatohepatitis (NASH), leading to faster fibrosis progression to end-stage liver disease and hepatocellular carcinoma, which are established risk factors of liver-related death(4-6).

One of the major gaps in clinical practice is the lack of safe and accurate methods that distinguish between patients with NASH, who are at risk of progression to advanced disease, from those who have simple steatosis and are less likely to develop liver-related complications(7). Timely identification of NASH before the onset of fibrosis would allow early intervention to avoid development of end-stage liver disease. Several biomarkers of inflammation have been evaluated, but they lack the accuracy and reliability necessary to eliminate the need for liver biopsy(8-13). Thus, diagnosis of NASH continues to rely on histologic evaluation of liver samples. However, liver biopsy is limited by the risk of complications, sampling bias and the inconvenience as a repeat measure of disease activity over time. Thus, innovative biomarkers to estimate the key histologic parameters for NASH diagnosis and disease monitoring in clinical trials and practice are urgently needed.

Magnetic resonance imaging (MRI) has advanced the evaluation of liver disease with techniques that accurately assess fibrosis - MR elastography (MRE)(14-16) and steatosis - MRI proton density fat fraction (MRI-PDFF)(17). MRE has emerged as the most accurate tool to predict hepatic fibrosis, with an AUROC above 0.90 for all fibrosis stages(18, 19) and higher accuracy than ultrasound-based elastography techniques (such as transient elastography or acoustic radiation force impulse elastography) for the detection of fibrosis in NAFLD(20-23). MRE has several advantages over ultrasound-based elastography, because it samples a much larger volume of the liver, it is not affected by body mass index(24) (25)or degree of steatosis(14), it is not operator dependent(26), it has favorable test-retest repeatability(26) and a high success rate(25),(27). MRE estimates liver stiffness, which

correlates to the amount of collagen deposition in the extracellular matrix, but liver stiffness is also influenced by other factors, such as inflammation, vascular congestion and cholestasis. Consequently, in early NASH when inflammation and cellular injury prevail over mild fibrosis, conventional 2D-MRE detects increased liver stiffness but cannot distinguish if the increase is due to viscoelastic changes of inflammation or due to mild fibrosis.

Recent preclinical studies have shown that varying the frequency of mechanical waves and using three-dimensional (3D) MRE software enables identification of MR parameters that are sensitive to early viscoelastic alterations in NASH before fibrosis onset. Compared to 2D-MRE, 3D-MRE allows a more comprehensive analysis of the steady-state dynamic shear wave propagation in the entire liver(28). In mouse models of diet-induced NASH, the *damping ratio* and *shear loss modulus* have been shown to enable discrimination of inflammation from fibrosis at early stages of disease, even before the development of histologically detectable necroinflammation and fibrosis(29). These data represent a strong scientific premise that warrants investigation of MRE as an imaging biomarker for the non-invasive detection of NASH in humans. If multifrequency 3D-MRE (mf3D-MRE) can be used to discriminate NASH from simple steatosis, it is conceivable that an imaging biomarker that combines mf3D-MRE for assessment of inflammation and ballooning with MRI-PDFF for assessment of steatosis could predict the histologic parameters of NASH and estimate disease activity by histologic NAFLD activity score (NAS) without the need for a liver biopsy.

Therefore, in this study we explored the performance of a novel MRI protocol that combines mf3D-MRE with MRI-PDFF and developed an imaging biomarker for NASH diagnosis and disease severity in obese human subjects at risk for NASH.

METHODS

Study subjects and design

The study included two cohorts of bariatric surgery candidates at risk for NASH: one prospective and one retrospective, as described below (cohort derivation flow in Supplemental Table 1).

To explore the imaging parameters of interest and the optimal frequency of vibration application of mechanical waves in humans, adult patients at risk for NASH were enrolled in a prospective clinical trial (NCT02565446(30)) (***prospective cohort***). The cohort consisted of consecutive obese patients who were evaluated for bariatric surgery between October 2015 and June 2017. Given the exploratory nature of the analysis without previous data or anticipated differences in the values of imaging parameters between NASH and non-NASH, a robust sample size calculation was not feasible. Based on previous MRE studies, where significant differences in liver stiffness correlating with NASH or fibrosis were noted at sample sizes of 48-58 subjects(14, 31), we aimed for a cohort of 80 subjects at risk for NASH. In order to account for unanticipated study events leading to incomplete data (conservatively estimated to occur in 30% of enrolled subjects), we aimed to enroll a total of 120 patients.

Exclusion criteria included excessive alcohol consumption (> 21 units/week for men and > 14 units/week for women), steatogenic medications (e.g. amiodarone, methotrexate, corticosteroids), presence of liver disease other than NAFLD, contraindications to MR imaging (claustrophobia, metallic aneurysm clips, spinal stimulators etc) or patients at high operative risk in whom a liver biopsy might lead to complications in the investigator's opinion. Patients who met the inclusion criteria underwent MR imaging per the protocol described below followed within 1 month by intraoperative core liver biopsy from the right lobe during the weight-reduction surgery.

After the optimal technical parameters for NASH detection were established using the prospective cohort, we took advantage of existing data from a retrospective cohort of bariatric surgical patients with NAFLD recruited at Mayo Clinic between March 2010 and May 2013, which has been previously described(24). This cohort had prospectively acquired clinical research data obtained through a similar protocol (mf3D-MRE/MRI-PDFF and intra-operative liver biopsy) with technical parameters similar to those identified in the first part of the analysis. The exclusion criteria were similar to those used for the exploratory cohort. Therefore, to increase the sample size and study power we combined the data from the 2 cohorts into a ***combined cohort*** which was used to develop a statistical model of histologic NASH prediction using the imaging parameters of interest.

MR imaging protocol

The imaging protocol consisted of mf3D-MRE to explore parameters that correlate with NASH, along with MRI-PDFF to estimate proton density fat fraction. MR examinations were performed on 1.5T whole-body scanners (GE Healthcare, Milwaukee, WI) at Mayo Clinic.

Multifrequency 3D-MRE imaging protocol: After a fasting period of at least 4 hours, patients were imaged in the supine position with the passive driver placed against the anterior body wall over the right lobe of the liver, held in place with an elastic band wrapped around the body. Continuous acoustic pressure waves were generated from an active driver, and were delivered to the passive driver via a 7.6-m long plastic tube. The waves were delivered at 3 separate frequencies (30, 40 and 60 Hz) in the prospective cohort and at 2 separate frequencies (40 and 60 Hz) in the retrospective cohort. The MRE acquisition was performed separately at each frequency as an axial multi-slice spin-echo echo-planar MRE sequence using three alternating orthogonal motion-encoding directions with a 72×72 in-plane acquisition matrix, repetition time of 1333-2666 ms, echo delay time of 43.7-57.0 ms, slice thickness of 3.5 mm, 44.8-cm FOV, 32 slices, a 250-kHz readout bandwidth, a parallel imaging acceleration factor of 3, and three evenly spaced phase offsets over one motion cycle. The encoded motion sensitivity was 8.3-13.4 μm/radian. 3D-MRE at each frequency was performed in three to six 20-second breath holds at the end of expiration.

Multifrequency 3D-MRE post-processing protocol: All 3D-MRE wave data were interpolated in-plane to 256×256 pixels and were (a) processed with the curl operator (using central differences), (b) processed with 20 evenly spaced 3D directional filters(32) (radial fourth-order Butterworth bandpass filter, cutoff frequencies of 0.000125 and 3 cm^{-1}), (c)

smoothed with a 3×3×3-pixel quartic kernel(33) , and (d) inverted with a direct inversion of the Helmholtz equation(34) to calculate the complex shear modulus G*= G' +i*G''. Several mechanical properties can be derived from G*, including the storage modulus (G'), loss modulus (G''), shear stiffness (|G*|), and the damping ratio (ζ = G''/(2*G')). For each subject, these quantities were reported as the mean and standard deviation of a single volumetric region of interest (ROI) manually drawn to encompass as much of the liver as possible that had substantial wave propagation based on visual evaluation by two experienced analysts (M.Y. and J.L.). The mean, standard deviation, median, and interquartile range were reported for all ROIs. The criteria for ROI placement were as follows: (a) include liver parenchyma only, (b) exclude regions without visually adequate magnitude of signal or shear wave amplitude, (c) stay two pixels away from the edges and exclude the top and bottom two slices of the liver, and (d) exclude unreliable measurements with the guidance of the confidence map that representing the reliability of the liver stiffness and damping ratio measurements at each voxel based on magnitude/phase signal to noise ratios.

MRI: Proton-density fat fraction was measured from a single 16-second breath-hold three-dimensional volumetric imaging sequence, which is a fast, spoiled, gradient echo sequence with a 256×160 prescribed in-plane acquisition matrix, TR = 13.0 ms, flip angle = 7°, slice thickness = 8 mm, 40-48 cm FOV, 28 slices, 83.33-kHz readout bandwidth. Six gradient echoes were applied to reconstruct water and fat images, relative fat fractions (PDFFs), and R2* maps (IDEAL-IQ, GE Healthcare). For each subject, PDFF and R2* measurements were reported as the mean of nine ROIs manually drawn in nine anatomic segments by two experienced analysts (S.K.V., M.L.W.)

Histologic assessment

All liver biopsy specimens were reviewed by Mayo Clinic liver pathologists as part of the clinical service. In addition, one study pathologist with NASH expertise provided a second interpretation while blinded to the results of the first interpretation and to imaging. For discrepancies in histologic NASH diagnosis in the prospective cohort (which occurred in 4 cases), the study pathologist reviewed the cases again and provided a final interpretation, while in the retrospective cohort a third pathologist was invited for review. NASH was defined histologically by the presence of steatosis with 1) hepatocellular ballooning or 2) lobular inflammation with associated fibrosis. The disease severity was estimated using the NAFLD activity score (NAS)(35).

Statistical analysis

Clinical, demographic, laboratory, imaging and histologic characteristics were compared between patients with and without NASH using Kruskal-Wallis rank sum test and Pearson's chi-squared test for continuous and categorical variables, respectively. We hypothesized that the three parameters of interest obtained from the pre-clinical studies, namely the *damping ratio* (DR), *shear stiffness* (SS) and *fat fraction* (FF) can be combined into a logistic regression model of histologic NASH prediction. We also evaluated the potential utility of other mf3D-MRE parameters, including attenuation, volumetric strain, storage modulus, loss

modulus and their standard deviations (as a measure of heterogeneity) in predicting histologic NASH using the lasso method(36).

Consequently, we explored the hypothesis derived from pre-clinical data that the DR obtained at lower frequency is superior to that obtained at the conventional 60 Hz frequency for NASH diagnosis. Logistic regression models including the DR at separate frequencies were compared in performance using c-statistics. After determining the optimal MRE frequency in the prospective cohort, we took advantage of a retrospective NAFLD cohort with similar data and combined the 2 cohorts into the *combined cohort*, from which a new, final logistic regression model was derived. We elected to use the 2 available cohorts by combining the data to increase the sample size and the predictive performance of the regression model, with cross-validation, as opposed to using one cohort for derivation and the other for validation, since the latter method is less robust due to smaller sample size. Among all the potential imaging parameters, the 3 parameters of interest were the most useful dimensions (they had the highest variance- Supplemental Methods), and this allowed combination of the 2 cohorts without concern for model overfitting. Although both DR and SS are calculated from storage modulus and loss modulus, the 2 parameters were obtained at different frequencies and there was no collinearity between them (Supplemental Methods).

Using the 3 parameters of interest at optimal frequencies, as determined in the first part of the analysis, we constructed two separate regression models, one for the prediction of NASH diagnosis (based on the pathologist's impression, not a NAS cut-off) as a binary outcome (yes/no) and one for the prediction of disease severity by NAS as a continuous scale with values ranging from 0 to 8. Model performance was estimated using c-statistics. Ten-fold cross-validation was performed for each of the 2 models and results were reported as cross-validated c-statistic. In order to compare the performance of the multiparametric biomarker to the currently available 2D MRE technology, we analyzed the predictive performance of shear stiffness values obtained at a frequency of 60Hz in a regression model using the combined cohort of bariatric patients. Statistical analyses were performed in SAS v9.4 (SAS Institute; Cary, NC) and R statistical software, version 3.2.0 (R Foundation for Statistical Computing, Vienna). The study was approved by the Institutional Review Board of Mayo Clinic. All authors had access to the study data and reviewed and approved the final manuscript.

RESULTS

Exploratory analysis of MRE parameters for NASH diagnosis

Prospective cohort—Among 120 patients enrolled in the prospective cohort, 32 were excluded due to incomplete data (liver biopsy was not performed due to complexity of the bariatric surgery: n=15; MRE was not performed due to claustrophobia: n=4, or terminated due to discomfort: n=1) or withdrawal for personal reasons of the participants (n=12). Of the 88 subjects who completed the study protocol, 70 (80%) were women, median age was 46, and 79 (90%) were white (Supplemental Table 2). The median time interval between liver biopsies and MRE was 7 (IQR=4-13) days. The median sample length was 1.7 (IQR=1.3-1.9) cm. NASH was diagnosed by histologic criteria in 37 (40%) of the subjects.

Only 3 subjects with NASH were found to have advanced fibrosis: stage 3 (n=2) and 4 (n=1).

There were significant differences in all the histologic parameters between NASH and non-NASH subjects (Supplemental Table 2). Similarly, there were significant differences in imaging parameters of interest between NASH and non-NASH subjects: DR at 40Hz and 60Hz, SS at 40Hz and 60Hz and fat fraction (Figure 1). None of the patients had significant iron overload. The R2* values were below 50ms.

Performance of multifrequency MRE for NASH diagnosis—None of the additional imaging parameters explored (attenuation, volumetric strain, storage modulus, loss modulus and their standard deviations), nor serologic parameters such as ALT, AST, fasting glucose, insulin, HOMA-IR, total cholesterol, LDL-cholesterol and triglycerides made a measureable improvement to a model using the primary three parameters of interest (DR, SS and FF) and were not included in further analysis (data not shown).

To explore the optimal frequency of applied MRE shear waves at which the DR best correlates with NASH, we explored several models using combinations of the parameters of interest with DR obtained at 30, 40 and 60 Hz, respectively (Table 1). Lowering the frequency to 40Hz optimized the DR estimation and improved the performance of histologic NASH prediction: cross-validated c-statistic=0.76 (95% CI 0.66-0.85). In Figure 2, the DR at 40 Hz decreases with the increase in lobular and portal inflammation and hepatocellular ballooning.

Development of an MRI-based prediction model of NASH diagnosis and NASH severity

Combined cohort—To increase the sample size and improve the study power, we added a retrospective cohort of 87 NAFLD patients with liver biopsy and mf3D-MRE at 40Hz and 60 Hz, which was previously described(24). The median time interval between liver biopsies and MRE was 27 (IQR=20-30) days. The sample length was 1.2 (IQR=0.9-1.7) cm. The imaging parameters were obtained using the same imaging protocol. After combining the prospective and retrospective subjects, the model derivation cohort consisted of 175 patients, median age 45, 141 (81%) women and 81 (46%) with histologic NASH (Table 2).

Model derivation—The 3 parameters of interest obtained from the combined cohort (DR at 40Hz, SS at 60Hz and FF) were included into a new logistic regression model of NASH prediction. The IQR-standardized model coefficients are shown in Table 3A. In this expanded cohort, the cross-validated c-statistic of model performance was 0.73 (95% CI 0.65-0.81), with sensitivity=0.67, specificity= 0.80, PPV= 0.73 and NPV=0.74 (Figure 3).

A separate logistic regression model for prediction of disease severity by NAS was developed using the same 3 imaging parameters of interest (Table 3B). The model cross-validated c-statistic was 0.82 (95% CI 0.77-0.87). An example output of the 2 models predicting NASH and NAS is shown in Figure 4: predicted probability of NASH as a binary outcome (yes/no) and predicted probabilities of each NAS value on a continuous scale ranging from 0 to 8 (the sum of all probabilities is 100). The highest probabilities within the 68% confidence interval were chosen to generate a range of predicted NAS score (shaded

area on the horizontal NAS bar). For example, in patient A, who by histology does not have NASH and whose NAS=0, the logistic regression model using imaging parameters predicted a 15% probability of NASH and a predicted NAS=0-1. Patient B, with histologic NASH and NAS=3, has a predicted probability of 60% for NASH and a predicted NAS=3-4. Lastly, patient C, with histologic NASH and NAS=6, has a 98% predicted probability of NASH and a predicted NAS=5-6.

In order to compare the performance of the multiparametric biomarker to the currently available 2D MRE technology, we analyzed the predictive performance of shear stiffness values obtained at a frequency of 60Hz in a regression model using the combined cohort of bariatric patients. The shear stiffness from 2D MRE predicted NASH with a cross-validated c-statistic of 0.61 (95% CI 0.53-0.69) and disease activity by NAS with a cross-validated c-statistic of 0.64 (95% CI 0.58-0.70).

DISCUSSION

In this work, we applied multiparametric MRI and MRE-based methods to noninvasively predict histologic findings in NASH. In this first step, we evaluated candidate MRI and MRE-based biomarkers in a well-characterized cohort of 175 obese subjects, using liver histology as reference. The results showed that within the 3 shear wave frequencies evaluated, 2 frequencies for acquiring stiffness and damping ratio provided the greatest ability to characterize NASH even in the absence of advanced fibrosis. If further validated, the ability to noninvasively assess NASH without a liver biopsy would represent an important advance in the field, with potential application in screening, disease monitoring and response to therapy in clinical practice and intervention trials.

We speculate that the frequency-dependent information provided by liver stiffness and damping ratio measurements is a reflection of inflammation (including associated edema and hyperemia) even in the absence of fibrosis. The damping ratio appears to decrease in NASH, and it best correlates with the disease when the mechanical stimuli are applied at lower frequency. It has potential diagnostic role in improving both the diagnosis accuracy of NASH and the performance of disease severity estimation, with a weight in the predictive model that is similar to that of shear stiffness. Whereas neither parameter alone has sufficient power to diagnose NASH, the combination of the 3D-MRE/MRI parameters provides good diagnostic discrimination of inflammation from simple steatosis. As fibrosis burden increases, the shear stiffness becomes the dominating imaging parameter.

As with most other diagnostic biomarkers, the performance of mf3D-MRE was developed in reference to the histological assessment of a liver biopsy sample. The volume of liver parenchyma assessed with a single 3D-MRE slice is approximately 1205 cm^3 at 40Hz, and 949 cm^3 at 60Hz, considerably higher than a single 2D-MRE slice (250 cm^3), or than the volume evaluated by shear wave elastography (20 cm^3), transient elastography (4 cm^3), and nearly 500-fold that of a liver biopsy (37, 38). Assessing a large volume of liver enables appreciation of spatial heterogeneity of parenchymal changes (39). Inflammation and hepatocellular ballooning can be focal, particularly in early disease stages, which leaves room for diagnostic inaccuracies by histology. Therefore, in evaluating the biomarker's

performance, this limitation of the “gold-standard” histologic diagnosis should be considered. Moreover, the inter-rater histologic agreement on NASH vs not NASH by different pathologists is 0.61(35). The weighted kappa statistics on steatosis, inflammation and ballooning grade are 0.84, 0.45 and 0.56, respectively, which suggests that the agreement of pathologists on grading the disease severity by NAS is equally imperfect. These issues further contribute to the imperfection of the gold-standard to which a biomarker is compared. These limitations create a “ceiling effect” on the maximal performance of any NASH biomarker, which cannot have a better discrimination than around 0.85.

The results of this study indicate that MRI and MRE-based biomarkers represent an improvement over the currently available data obtained from conventional 2D-MRE and have potential to fill important gaps in several circumstances. As the only noninvasive biomarker that predicts disease severity by NAS, mf3D-MRE could be applied in *risk-stratification* of patients with NASH. Patients without advanced fibrosis, but with high disease activity based on the predicted NAS, can be appropriately counseled about the risk of disease progression and advised to implement aggressive therapeutic interventions. Moreover, mf3D-MRE might be considered for use as a *surrogate end-point* in interventional clinical trials, because it offers the advantage to predict not only NAS (the most commonly used surrogate end-point in NASH trials), but also separate estimations of the three components of NAS (steatosis, inflammation/ballooning and fibrosis), which are individually targeted in certain experimental monotherapies.

Accordingly, this provides motivation for further studies to evaluate the role of mf3D-MRE as a screening tool in selected patients at risk for NASH, such as those with severe obesity, diabetes or metabolic syndrome. One of its most important performance characteristics is the high specificity of 80%, which is advantageous for the identification of individuals with simple steatosis by ruling out those with NASH. Recognizing the low risk of future liver disease for individuals with simple steatosis and focusing on those with NASH will allow for a more targeted therapeutic approach and prevent downstream costs and unnecessary healthcare resources in a disease with significant economic burden(40).

The strengths of this study include the innovative approach, a large, rigorously characterized population at risk for NASH using the gold-standard method of NASH diagnosis by histology, with uniform interpretation by one study pathologist. We targeted individuals with early NASH, without advanced fibrosis, and this criterion was met by the vast majority of the subjects. Limitations include the severe obesity, female predominance and the mild-moderate disease severity, with few subjects having high NAS. Whereas this cohort with severe obesity may not be fully representative of the typical NAFLD population, it provided a more suitable venue to obtain liver biopsies in a controlled operative environment from a large number of patients. Like many other studies of bariatric surgery patients(41),(42),(43), this cohort provides the opportunity to derive important data in the field of fatty liver disease, that NASH can be diagnosed non-invasively by MRE. However, future work should test the generalizability of mf3D-MRE as an accurate NASH biomarker by validating these results in a population with lower BMI ranges and more severe steatohepatitis, and assess its cost-effectiveness and role in disease monitoring. The MRE analysis used in this study

employed manual selection of the region of interest leading to potential interobserver variability(26). A confidence map calculated during the mechanical properties inversion was available to guide manual ROI selection to mitigate inter-reader variation. Future studies should address the utility of automated liver elasticity calculation (44). Similarly, studies comparing the performance using different field strengths (1.5T vs. 3T) should be performed.

Noninvasive detection of NASH and accurate determination of fibrosis stage remain key diagnostic challenges. The technical approach tested in this study combines mf3D-MRE and MRI-PDFF in a single test that has the potential to provide a comprehensive estimation of inflammation, ballooning, steatosis and fibrosis in one setting. Moreover, it is an accurate imaging biomarker not only for NASH diagnosis, but also for estimation of disease severity. The value of histological assessment in liver disease remains unquestioned, but by providing equivalent information regarding the state of the liver parenchyma, mf3D-MRE has the potential to obviate the limitations of liver biopsy in the management of NAFLD.

Supplementary Material

Refer to Web version on PubMed Central for supplementary material.

Acknowledgments

Grant support

Alina M. Allen: National Institute of Diabetes and Digestive and Kidney Diseases (K23DK115594); Mayo Clinic Center for Cell Signaling in Gastroenterology (NIDDK P30DK084567); American College of Gastroenterology 2017 Junior Faculty Development Grant. Mayo Clinic Transform the Practice Grant.

Meng Yin: National Institutes of Health (EB017197); Mayo Clinic Center for Individualized Medicine Imaging Biomarker Discovery Program.

Richard L. Ehman: National Institutes of Health (EB001981).

Vijay H. Shah: National Institute on Alcohol Abuse and Alcoholism (AA021171).

Abbreviations

2D	two-dimensional
3D	three-dimensional
DR	damping ratio
FF	fat fraction
Hz	hertz
MRE	magnetic resonance elastography
mf3D-MRE	multifrequency 3D-MRE
MRI	magnetic resonance imaging

MRI-PDFF	MRI proton density fat fraction
NAFLD	nonalcoholic fatty liver disease
NASH	nonalcoholic steatohepatitis
NPV	negative predictive value
PPV	positive predictive value
SS	shear stiffness

REFERENCES

1. Case A, Deaton A. Rising morbidity and mortality in midlife among white non-Hispanic Americans in the 21st century. Proc Natl Acad Sci U S A 2015;112:15078–15083. [PubMed: 26575631]
2. Younossi ZM, Koenig AB, Abdelatif D, Fazel Y, Henry L, Wymer M. Global epidemiology of nonalcoholic fatty liver disease-Meta-analytic assessment of prevalence, incidence, and outcomes. Hepatology 2016;64:73–84. [PubMed: 26707365]
3. Allen AM, Therneau TM, Larson JJ, Coward A, Somers VK, Kamath PS. Nonalcoholic fatty liver disease incidence and impact on metabolic burden and death: A 20 year-community study. Hepatology 2018;67:1726–1736. [PubMed: 28941364]
4. Angulo P, Kleiner DE, Dam-Larsen S, Adams LA, Bjornsson ES, Charatcharoenwitthaya P, Mills PR, et al. Liver Fibrosis, but No Other Histologic Features, Is Associated With Long-term Outcomes of Patients With Nonalcoholic Fatty Liver Disease. Gastroenterology 2015;149:389–397.e310. [PubMed: 25935633]
5. Dam-Larsen S, Franzmann M, Andersen IB, Christoffersen P, Jensen LB, Sorensen TI, Becker U, et al. Long term prognosis of fatty liver: risk of chronic liver disease and death. Gut 2004;53:750–755. [PubMed: 15082596]
6. Ekstedt M, Franzen LE, Mathiesen UL, Thorelius L, Holmqvist M, Bodemar G, Kechagias S. Long-term follow-up of patients with NAFLD and elevated liver enzymes. Hepatology 2006;44:865–873. [PubMed: 17006923]
7. Singh S, Allen AM, Wang Z, Prokop LJ, Murad MH, Loomba R. Fibrosis progression in nonalcoholic fatty liver vs nonalcoholic steatohepatitis: a systematic review and meta-analysis of paired-biopsy studies. Clin Gastroenterol Hepatol 2015;13:643–654.e641-649; quiz e639-640. [PubMed: 24768810]
8. Poynard T, Ratziu V, Charlotte F, Messous D, Munteanu M, Imbert-Bismut F, Massard J, et al. Diagnostic value of biochemical markers (NashTest) for the prediction of non alcoholo steato hepatitis in patients with non-alcoholic fatty liver disease. BMC Gastroenterol 2006;6:34. [PubMed: 17096854]
9. Munteanu M, Tiniakos D, Anstee Q, Charlotte F, Marchesini G, Bugianesi E, Trauner M, et al. Diagnostic performance of FibroTest, SteatoTest and ActiTest in patients with NAFLD using the SAF score as histological reference. Aliment Pharmacol Ther 2016;44:877–889. [PubMed: 27549244]
10. Hui JM, Farrell GC, Kench JG, George J. High sensitivity C-reactive protein values do not reliably predict the severity of histological changes in NAFLD. Hepatology 2004;39:1458–1459. [PubMed: 15122781]
11. Feldstein AE, Wieckowska A, Lopez AR, Liu YC, Zein NN, McCullough AJ. Cytokeratin-18 fragment levels as noninvasive biomarkers for nonalcoholic steatohepatitis: a multicenter validation study. Hepatology 2009;50:1072–1078. [PubMed: 19585618]
12. Cusi K, Chang Z, Harrison S, Lomonaco R, Bril F, Orsak B, Ortiz-Lopez C, et al. Limited value of plasma cytokeratin-18 as a biomarker for NASH and fibrosis in patients with non-alcoholic fatty liver disease. J Hepatol 2014;60:167–174. [PubMed: 23973932]

13. Loomba R, Quehenberger O, Armando A, Dennis EA. Polyunsaturated fatty acid metabolites as novel lipidomic biomarkers for noninvasive diagnosis of nonalcoholic steatohepatitis. J Lipid Res 2015;56:185–192. [PubMed: 25404585]
14. Yin M, Talwalkar JA, Glaser KJ, Manduca A, Grimm RC, Rossman PJ, Fidler JL, et al. Assessment of hepatic fibrosis with magnetic resonance elastography. Clin Gastroenterol Hepatol 2007;5:1207–1213.e1202. [PubMed: 17916548]
15. Kim D, Kim WR, Talwalkar JA, Kim HJ, Ehman RL. Advanced fibrosis in nonalcoholic fatty liver disease: noninvasive assessment with MR elastography. Radiology 2013;268:411–419. [PubMed: 23564711]
16. Dulai PS, Sirlin CB, Loomba R. MRI and MRE for non-invasive quantitative assessment of hepatic steatosis and fibrosis in NAFLD and NASH: Clinical trials to clinical practice. J Hepatol 2016;65:1006–1016. [PubMed: 27312947]
17. Noureddin M, Lam J, Peterson MR, Middleton M, Hamilton G, Le TA, Bettencourt R, et al. Utility of magnetic resonance imaging versus histology for quantifying changes in liver fat in nonalcoholic fatty liver disease trials. Hepatology 2013;58:1930–1940. [PubMed: 23696515]
18. Loomba R, Wolfson T, Ang B, Hooker J, Behling C, Peterson M, Valasek M, et al. Magnetic resonance elastography predicts advanced fibrosis in patients with nonalcoholic fatty liver disease: a prospective study. Hepatology 2014;60:1920–1928. [PubMed: 25103310]
19. Singh S, Venkatesh SK, Loomba R, Wang Z, Sirlin C, Chen J, Yin M, et al. Magnetic resonance elastography for staging liver fibrosis in non-alcoholic fatty liver disease: a diagnostic accuracy systematic review and individual participant data pooled analysis. Eur Radiol 2016;26:1431–1440. [PubMed: 26314479]
20. Imajo K, Kessoku T, Honda Y, Tomeno W, Ogawa Y, Mawatari H, Fujita K, et al. Magnetic Resonance Imaging More Accurately Classifies Steatosis and Fibrosis in Patients With Nonalcoholic Fatty Liver Disease Than Transient Elastography. Gastroenterology 2016;150:626–637.e627. [PubMed: 26677985]
21. Park CC, Nguyen P, Hernandez C, Bettencourt R, Ramirez K, Fortney L, Hooker J, et al. Magnetic Resonance Elastography vs Transient Elastography in Detection of Fibrosis and Noninvasive Measurement of Steatosis in Patients With Biopsy-Proven Nonalcoholic Fatty Liver Disease. Gastroenterology 2017;152:598–607.e592. [PubMed: 27911262]
22. Cui J, Heba E, Hernandez C, Haufe W, Hooker J, Andre MP, Valasek MA, et al. Magnetic resonance elastography is superior to acoustic radiation force impulse for the Diagnosis of fibrosis in patients with biopsy-proven nonalcoholic fatty liver disease: A prospective study. Hepatology 2016;63:453–461. [PubMed: 26560734]
23. Yoon JH, Lee JM, Woo HS, Yu MH, Joo I, Lee ES, Sohn JY, et al. Staging of hepatic fibrosis: comparison of magnetic resonance elastography and shear wave elastography in the same individuals. Korean J Radiol 2013;14:202–212. [PubMed: 23483022]
24. Chen J, Yin M, Talwalkar JA, Oudry J, Glaser KJ, Smyrk TC, Miette V, et al. Diagnostic Performance of MR Elastography and Vibration-controlled Transient Elastography in the Detection of Hepatic Fibrosis in Patients with Severe to Morbid Obesity. Radiology 2017;283:418–428. [PubMed: 27861111]
25. Yin M, Glaser KJ, Talwalkar JA, Chen J, Manduca A, Ehman RL. Hepatic MR Elastography: Clinical Performance in a Series of 1377 Consecutive Examinations. Radiology 2016;278:114–124. [PubMed: 26162026]
26. Shire NJ, Yin M, Chen J, Railkar RA, Fox-Bosetti S, Johnson SM, Beals CR, et al. Test-retest repeatability of MR elastography for noninvasive liver fibrosis assessment in hepatitis C. J Magn Reson Imaging 2011;34:947–955. [PubMed: 21751289]
27. Wagner M, Corcuera-Solano I, Lo G, Esses S, Liao J, Besa C, Chen N, et al. Technical Failure of MR Elastography Examinations of the Liver: Experience from a Large Single-Center Study. Radiology 2017;284:401–412. [PubMed: 28045604]
28. Loomba R, Cui J, Wolfson T, Haufe W, Hooker J, Szeverenyi N, Ang B, et al. Novel 3D Magnetic Resonance Elastography for the Noninvasive Diagnosis of Advanced Fibrosis in NAFLD: A Prospective Study. Am J Gastroenterol 2016;111:986–994. [PubMed: 27002798]

29. Yin M, Glaser KJ, Manduca A, Mounajjed T, Malhi H, Simonetto DA, Wang R, et al. Distinguishing between Hepatic Inflammation and Fibrosis with MR Elastography. Radiology 2017;284:694–705. [PubMed: 28128707]
30. ClinicalTrials.gov.In.
31. Chen J, Talwalkar JA, Yin M, Glaser KJ, Sanderson SO, Ehman RL. Early detection of nonalcoholic steatohepatitis in patients with nonalcoholic fatty liver disease by using MR elastography. Radiology 2011;259:749–756. [PubMed: 21460032]
32. Manduca A, Lake DS, Kruse SA, Ehman RL. Spatio-temporal directional filtering for improved inversion of MR elastography images. Med Image Anal 2003;7:465–473. [PubMed: 14561551]
33. Romano AJ, Bucaro JA, Ehnan RL, Shirron JJ. Evaluation of a material parameter extraction algorithm using MRI-based displacement measurements. IEEE Trans Ultrason Ferroelectr Freq Control 2000;47:1575–1581. [PubMed: 18238703]
34. Manduca A, Oliphant TE, Dresner MA, Mahowald JL, Kruse SA, Amromin E, Felmlee JP, et al. Magnetic resonance elastography: non-invasive mapping of tissue elasticity. Med Image Anal 2001;5:237–254. [PubMed: 11731304]
35. Kleiner DE, Brunt EM, Van Natta M, Behling C, Contos MJ, Cummings OW, Ferrell LD, et al. Design and validation of a histological scoring system for nonalcoholic fatty liver disease. Hepatology 2005;41:1313–1321. [PubMed: 15915461]
36. Tibshirani R Regression Shrinkage and Selection via the lasso. Journal of the Royal Statistical Society. Series B 1996.
37. Barr RG, Ferraioli G, Palmeri ML, Goodman ZD, Garcia-Tsao G, Rubin J, Garra B, et al. Elastography Assessment of Liver Fibrosis: Society of Radiologists in Ultrasound Consensus Conference Statement. Radiology 2015;276:845–861. [PubMed: 26079489]
38. Bravo AA, Sheth SG, Chopra S. Liver biopsy. N Engl J Med 2001;344:495–500. [PubMed: 11172192]
39. Venkatesh SK, Wells ML, Miller FH, Jhaveri KS, Silva AC, Taouli B, Ehman RL. Magnetic resonance elastography: beyond liver fibrosis-a case-based pictorial review. Abdom Radiol (NY) 2017.
40. Allen AM, Van Houten HK, Sangaralingham LR, Talwalkar JA, McCoy RG. Healthcare Cost and Utilization in Nonalcoholic Fatty Liver Disease: Real-World Data from a Large US Claims Database. Hepatology 2018.
41. Lassailly G, Caiazzo R, Buob D, Pigeyre M, Verkindt H, Labreuche J, Raverdy V, et al. Bariatric Surgery Reduces Features of Nonalcoholic Steatohepatitis in Morbidly Obese Patients. Gastroenterology 2015;149:379–388; quiz e315-376. [PubMed: 25917783]
42. Mathurin P, Hollebecque A, Arnalsteen L, Buob D, Leteurtre E, Caiazzo R, Pigeyre M, et al. Prospective study of the long-term effects of bariatric surgery on liver injury in patients without advanced disease. Gastroenterology 2009;137:532–540. [PubMed: 19409898]
43. Poynard T, Lassailly G, Diaz E, Clement K, Caiazzo R, Tordjman J, Munteanu M, et al. Performance of biomarkers FibroTest, ActiTest, SteatoTest, and NashTest in patients with severe obesity: meta analysis of individual patient data. PLoS One 2012;7:e30325. [PubMed: 22431959]
44. Dzyubak B, Venkatesh SK, Manduca A, Glaser KJ, Ehman RL. Automated liver elasticity calculation for MR elastography. J Magn Reson Imaging 2016;43:1055–1063. [PubMed: 26494224]

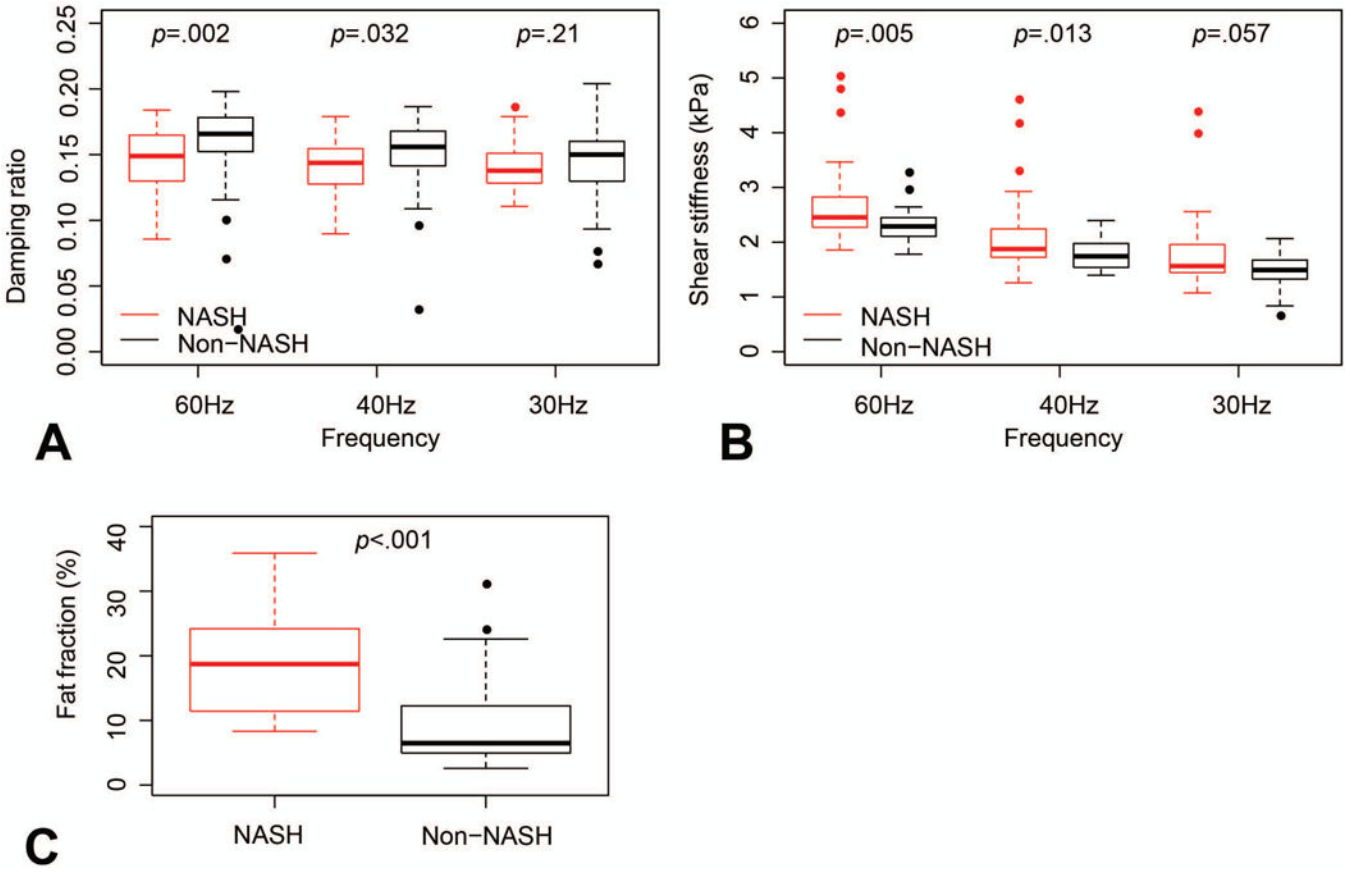

FIGURE 1. Imaging parameters of interest in patients with NASH versus non-NASH.

A. Damping ratio derived from 3D-MRE at 60Hz, 40Hz and 30Hz. Significant differences between NASH and non-NASH were noted at 40Hz and 60Hz. **B.** Shear stiffness (kPa) derived from 3D-MRE at 60Hz, 40Hz and 30Hz. Significant differences between NASH and non-NASH were noted at 40Hz and 60Hz. **C.** Fat fraction (%) derived from MRI-PDFF was significantly higher in NASH versus non-NASH patients.

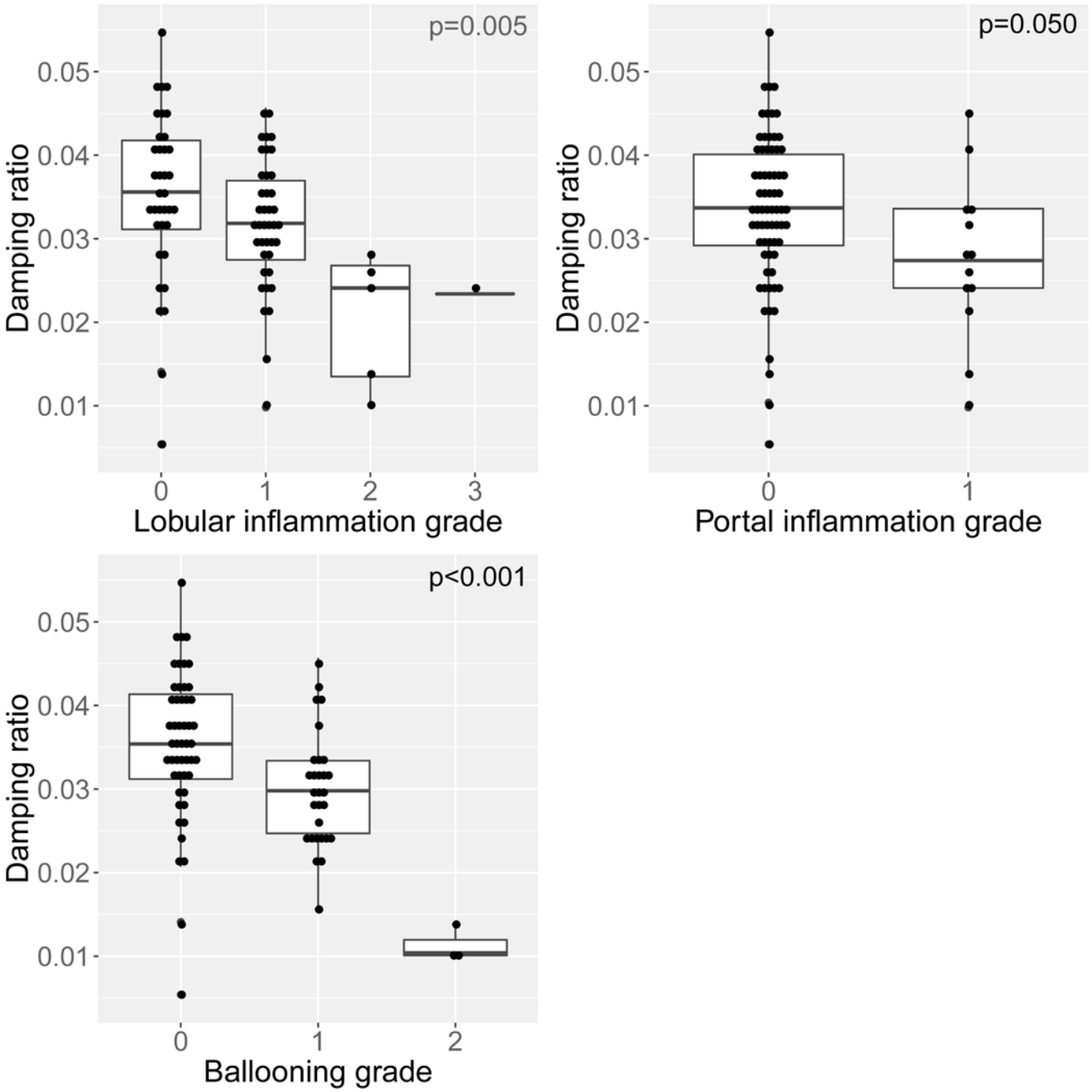

FIGURE 2.
The correlation of damping ratio values with histologic parameters of nonalcoholic steatohepatitis.

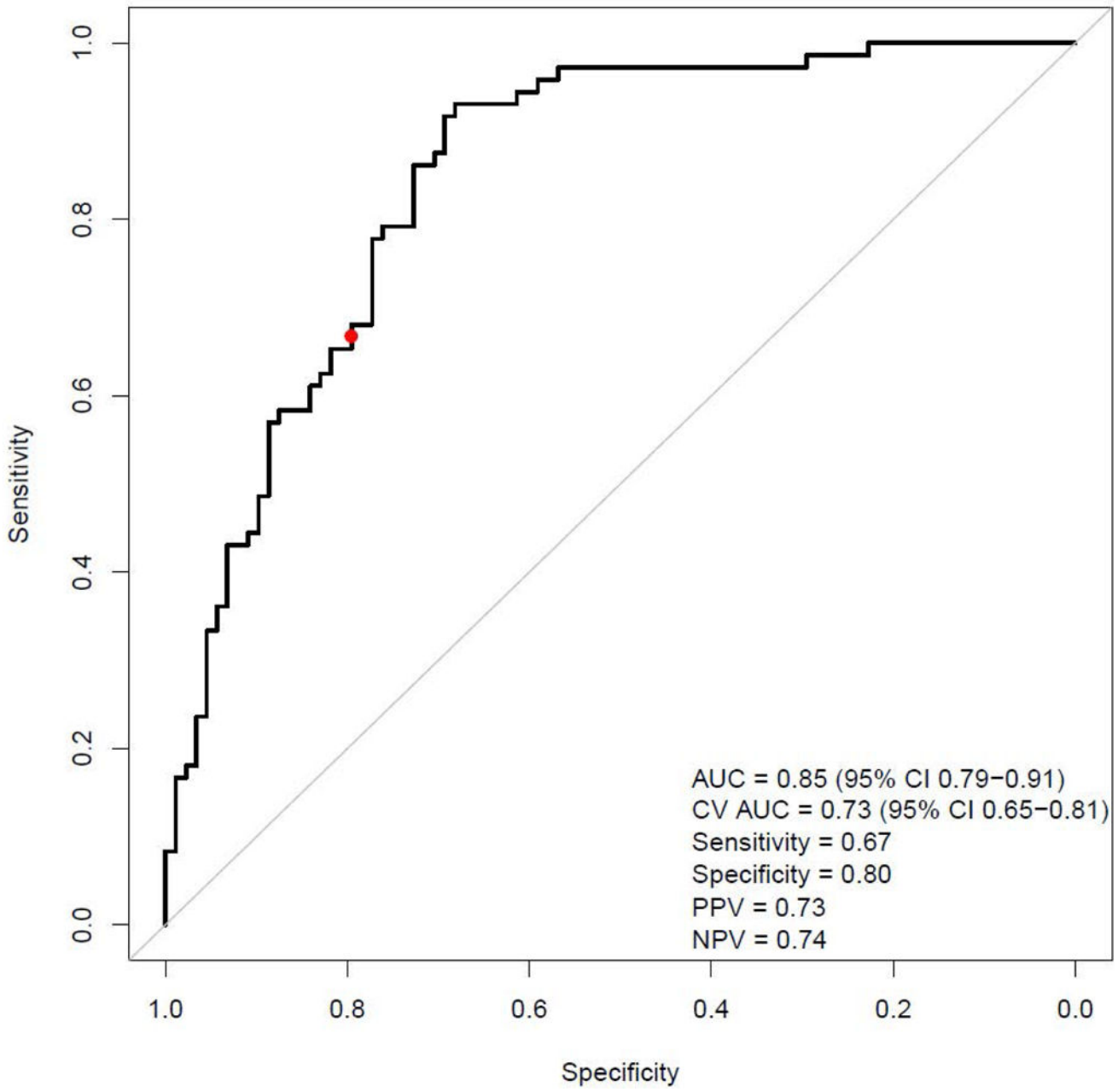

FIGURE 3. Predictive performance of the imaging biomarker for NASH diagnosis.
AUC: area under the curve; PPV: positive predictive value; NPV: negative predictive value.

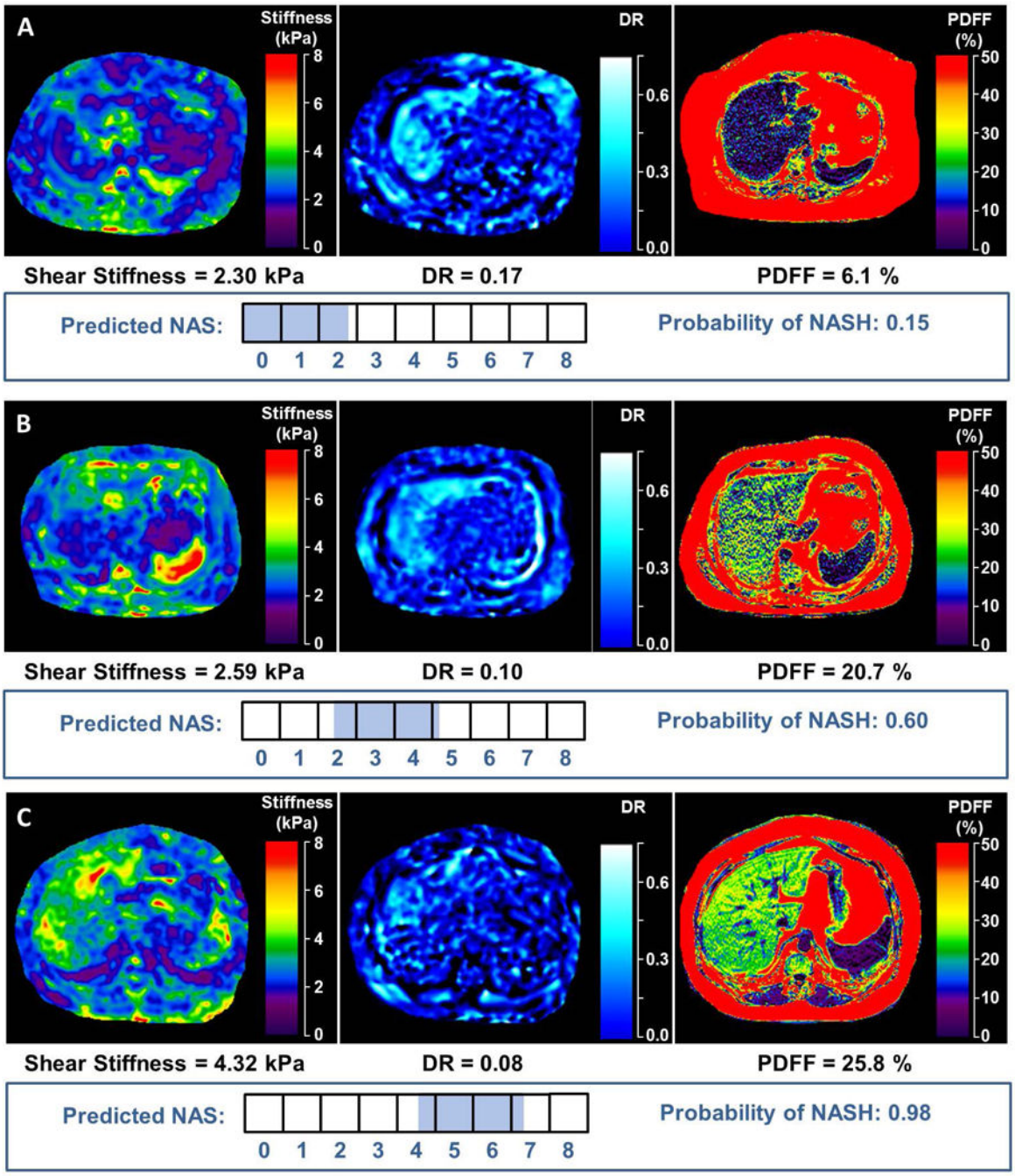

FIGURE 4. Examples of imaging analyses and predicted probabilities of NASH and NAFLD activity score (NAS) from three study patients.

The 3 imaging parameters included in the predictive model are shown: mf3D-MRE depiction of shear stiffness and damping ratio; MRI-PDFF depiction of fat fraction. The horizontal boxes illustrate the NAS values ranging from 0-8. The shaded part of the boxes represents the predicted range of NAS which were derived from the regression model as the highest probabilities within the 68% confidence interval. In patient A, who by histology does not have NASH and whose NAS=0, the logistic regression model using imaging parameters predicted a 15% probability of NASH and a predicted NAS=0-1. Patient B, with

histologic NASH and NAS=3, has a predicted probability of 60% for NASH and a predicted NAS=3-4. Lastly, patient C, with histologic NASH and NAS=6, has a 98% predicted probability of NASH and a predicted NAS=5-6.

Table 1.

Model performance for NASH prediction in the exploratory cohort of 88 bariatric subjects using mf3D MRE at 30, 40 and 60 Hz.

Imaging parameters included in each model	Model performance for histologic NASH prediction	
	c-statistic (95% CI)	Cross-validation c-statistic (95% CI)
DR-60 Hz, SS-60 Hz, FF	0.87 (0.79, 0.95)	0.74 (0.64, 0.83)
DR-40 Hz, SS-60 Hz, FF	0.87 (0.79, 0.95)	0.76 (0.66, 0.85)
DR-30 Hz, SS-60 Hz, FF	0.87 (0.79, 0.95)	0.74 (0.65, 0.84)

Table 2.

Characteristics of the combined cohorts of bariatric surgery candidates used for final statistical model derivation.

		NASH N=81	Not NASH N=94	p-value
Age, median (IQR)		47 (39-58)	45 (39-55)	0.65
Female- n (%)		51 (64%)	77 (83%)	0.008
BMI, median (IQR)		46 (41-57)	45 (42-49)	0.39
ALT, median (IQR)		37 (29-53)	22 (18-30)	<0.001
AST, median (IQR)		28 (24-38)	22 (19-28)	<0.001
Histologic parameters				
Steatosis grade	0	1 (1%)	37 (39%)	<0.001
	1	38 (48%)	49 (52%)	
	2	25 (31%)	6 (6%)	
	3	16 (20%)	2 (2%)	
Lobular inflammation grade	0	3 (4%)	64 (68%)	<0.001
	1	64 (79%)	29 (31%)	
	2	13 (16%)	1 (1%)	
	3	1 (1%)	0 (0%)	
Hepatocyte ballooning grade	0	13 (16%)	92 (98%)	<0.001
	1	50 (63%)	2 (2%)	
	2	17 (21%)	0 (0%)	
Fibrosis stage	0	14 (17%)	83 (88%)	<0.001
	1	33 (41%)	6 (6%)	
	2	18 (22%)	4 (4%)	
	3	7 (9%)	0 (0%)	
	4	9 (11%)	1 (1%)	
Histologic NAFLD activity score (NAS)	0	0 (0%)	28 (30%)	<0.001
	1	1 (1%)	38 (40%)	
	2	6 (7%)	22 (23%)	
	3	24 (30%)	6 (6%)	
	4	30 (37%)	0 (0%)	
	5	13 (16%)	0 (0%)	
	6	5 (6%)	0 (0%)	
	7	2 (3%)	0 (0%)	
	8	0 (0%)	0 (0%)	

Table 3.

Model coefficients derived from logistic regression for NASH prediction (A) and ordinal logistic regression for NAFLD activity score prediction (B).

A. Prediction of NASH diagnosis			
Parameter	**Coefficient (per IQR)**	**Standard error**	**p value**
DR-40	0.37	0.33	0.26
SS-60	0.75	0.21	<0.001
FF	1.73	0.34	<0.001

B. Prediction of NAFLD activity score (NAS)			
Parameter	**Coefficient (per IQR)**	**Standard error**	**p value**
DR-40	0.70	0.25	0.004
SS-60	0.64	0.10	<0.001
FF	2.46	0.29	<0.001